Dynamics of Spontaneous Otoacoustic Emissions

Christopher Bergevin and Anthony Salerno

Department of Physics & Astronomy, York University, Canada

Abstract.
Spontaneous otoacoustic emissions (SOAEs) have become a hallmark feature in modern theories of an 'active' inner ear, given their numerous correlations to auditory function (e.g., threshold microstructure, neurophysiological tuning curves), near universality across tetrapod classes, and physiological correlates at the single hair cell level. However, while several different classes of nonlinear models exist that describe the mechanisms underlying SOAE generation (e.g., coupled limit-cycle oscillators, global standing waves), there is still disagreement as to precisely which biophysical concepts are at work. Such is further compounded by the idiosyncratic nature of SOAEs: Not all ears emit, and when present, SOAE activity can occur at seemingly arbitrary frequencies (though always within the most sensitive range of the audiogram) and in several forms (e.g., peaks, broad 'baseline' plateaus). The goal of the present study was to develop new signal processing and stimulation techniques that would allow for novel features of SOAE activity to be revealed. To this end, we analyzed data from a variety of different species: human, lizard, and owl. First, we explored several strategies for examining SOAE waveforms in the absence of external stimuli to further ascertain what constitutes 'self-sustained sinusoids' versus 'filtered noise'. We found that seemingly similar peaks in the spectral domain could exhibit key differences in the time domain, which we interpret as providing critical information about the underlying oscillators and their coupling. Second, we introduced dynamic stimuli (swept-tones, tone bursts) at a range of levels, whose interaction with SOAEs could be visualized in the time-frequency domain. Aside from offering a readily accessible way to visualize many previously reported effects (e.g., entrainment, facilitation), we observed several new features such as subharmonic distortion generation and competing pulling/pushing effects when multiple tones were present. Furthermore, the tone burst data provide quantitative bounds on the dynamics of the relaxation oscillations. These data should provide new insights into how precisely how SOAE generators are related to (the more commonly measured) OAEs evoked via external stimuli and presumably speak to the robustness of the hair cell as the underlying basis for SOAE activity.

INTRODUCTION

Although numerous theoretical studies have explored the basis for spontaneous otoacoustic emission (SOAE) generation (e.g. [4, 8, 10, 14]), there is still uncertainty with regard to how microscopic (i.e., individual hair cell) and macroscopic scales (i.e., the ear as a system) come together. This bridge is important, as it serves to elucidate the dual role of a single hair cell as as an auditory filter (i.e., transducer) and as the fundamental 'active' (i.e., power amplification) element embedded into a system. Presumably, many of the remarkable properties of the ear likely emerge collectively. For example, models that consider an SOAE generator as a 'noise-perturbed limit cycle oscillator' [12] could be extended to capture the likely scenario that a given 'generator' is likely in fact itself a collection of coupled nonlinear oscillators (e.g., [14]).

Motivated by previous studies elucidating SOAE properties beyond just averaged spectra as shown in Fig.1 (left column) [1, 3, 9–13, 15], we attempt here to explore new strategies to examine and stimulate SOAE activity. The ultimate goal is to better understand how the underlying hair cells might behave as independent limit cycle oscillators and how they collectively interact to form the summed SOAE response measurable at the external auditory meatus. To this end, we present data from several different vertebrate species where the morphology differs significantly (e.g., structure of the tectorial membrane) to explore implications for hair cell–hair cell coupling. Our focus is upon 'dynamic' properties; that is, how various aspects change with respect to time (on short & long scales), both with and without an external stimulus.

METHODS

SOAE recordings were made in a double-walled sound-attenuated booth (IAC) using an Etymotic ER-10C connected to a Lynx Two-A sound card (Lynx Studio Technology) using a 44.1 kHz sample rate and controlled using custom software. For lizard and owl recordings, animals were lightly anesthetized and kept at a stable body temperature via

a heating blanket. All lizard data shown here come from *Anolis carolinensis*[1]. In cases where external stimuli were presented, the earphones were calibrated in-situ using flat-spectrum random phase noise. All analysis was performed using custom software written in Matlab.

With regard to Fig.1, the left column represents spectrally-averaged responses of 400 segments, each 8192 points long, taken sequentially from a single artifact-free waveform (typically 120 s long). For data shown in the center and right columns, the Fourier transform of the entire waveform was filtered in the spectral domain using a recursive exponential filter centered about the peak of interest. The filter bandwidth was chosen to be narrow enough to just capture all energy associated with the peak. The data were then inverse transformed back to the time domain. Subsequently, either the analytic signal was computed via the Hilbert transform (middle column) or the amplitude distribution computed for short segments (right column). Another analysis approach employed to examine responses to external stimuli (e.g., Figs.2 and 3) was a short-time Fourier transform (STFT), commonly used to generate spectrograms (see [6]).

RESULTS

Statistical properties. As shown in Fig.1, a variety of SOAE spectra can be observed in different types of ears. Humans typically show an idiosyncratic array of peaks (if any), while the owl and lizard tend to have a more orderly distribution. Furthermore, lizards commonly have a broad 'baseline' apparent, upon which the peaks sit atop (e.g., 2-4 kHz in Fig.1G) [7]. Such also appears present in the owl to a more limited extent. With regard to individual peaks, properties (Fig.1, middle column) can indicate relatively stable sinusoids (sharp ring shape seen for human data) to responses more dominated by noise (diffuse ring for owl data). For humans and lizards, large spectral peaks typically had properties (to a varying degree) consistent with an underlying sinusoid. In contrast for the owl, sharp spectral peaks typically were highly noisy. Smaller peaks for the owl typically show distributions entirely dominated by noise (i.e., centroids rather than rings).

The time course of the amplitude distribution (Fig.1, right column) is particularly telling: envelope fluctuations can be distinguished from instances where a given emission peak appears to turn off (e.g., [3]). Note that for the (arbitrarily chosen) interval shown in Fig.1I, the lizard's SOAE peak appears to exhibit a region where the emission turns off for $\sim$20 ms (around the 0.07 s mark). The noisy distributions for the owl do not appear to be associated with a mechanism of turning on/off, at least for the time scale shown.

Interactions with external stimuli. When using the STFT to examine the effects of swept tones (Fig.2), SOAEs appear as horizontal bands while the stimulus appears as the diagonal trace. Regions of 'suppression' are clearly apparent about the tone, as are areas of facilitation (i.e., localized magnitude increases) and frequency pushing/pulling as the tone moves towards/away from a given SOAE peak. Also visible are regions of subharmonic distortion: when the tone frequency matches that of a relatively large amplitude SOAE and there is another peak at half that frequency, facilitation can occur (e.g., 1.95 kHz peak at $\sim$2.95 s mark in bottom left panel of Fig.2). When two tones were present, similar effects were observed with strong regions of facilitation between the tones. Smaller frequency separations (fixed value or ratio) resulted in greater intermodulation distortions (e.g., $2f_1 - f_2$) becoming apparent.

For the swept tones shown in Fig.2, changing either the sweep rate or direction had little effect, indicating these responses can be effectively considered in steady-state. To circumvent this, we presented cosine-ramped tone bursts as shown in Fig.3. The bursts cause spectrally and temporally localized regions of 'suppression' (appearing as vertical stripes), with relatively fast dynamics. That is, the SOAE peaks transition into a steady-state behavior quickly compared to the time–frequency resolution employed in the current analysis. We note there appears a longer delay between burst and subsequent suppression (if any) for the human (e.g., Fig.3A, $\sim$1.9 s mark for the 2.18 kHz peak) compared to the lizard. To better assess the dynamics, the center and right panels of Fig.3 provide alternative views. For example, there appears a non-monotonic relationship with regard to the degree of suppression relative to proximity of the SOAE peak frequency, though this could possibly be attributed to spectral splatter from the stimulus.

Lastly, these data indicate various degrees of stability in SOAE patterns in the absence of external stimuli. Over short timescales, Fig.1 demonstrates envelope fluctuations for individual peaks. Over much longer periods of time, the left panel of Fig.2 shows that the the overall SOAE spectra shape in lizards is preserved across $\sim$ 3.3 months. While some differences are apparent, such might be attributable to the body temperature not being strictly the same in both sessions.

[1] This lizard species has auditory papilla that contains approximately 160 hair cells total and lacks a tectorial membrane over the majority of it, unlike the human or owl.

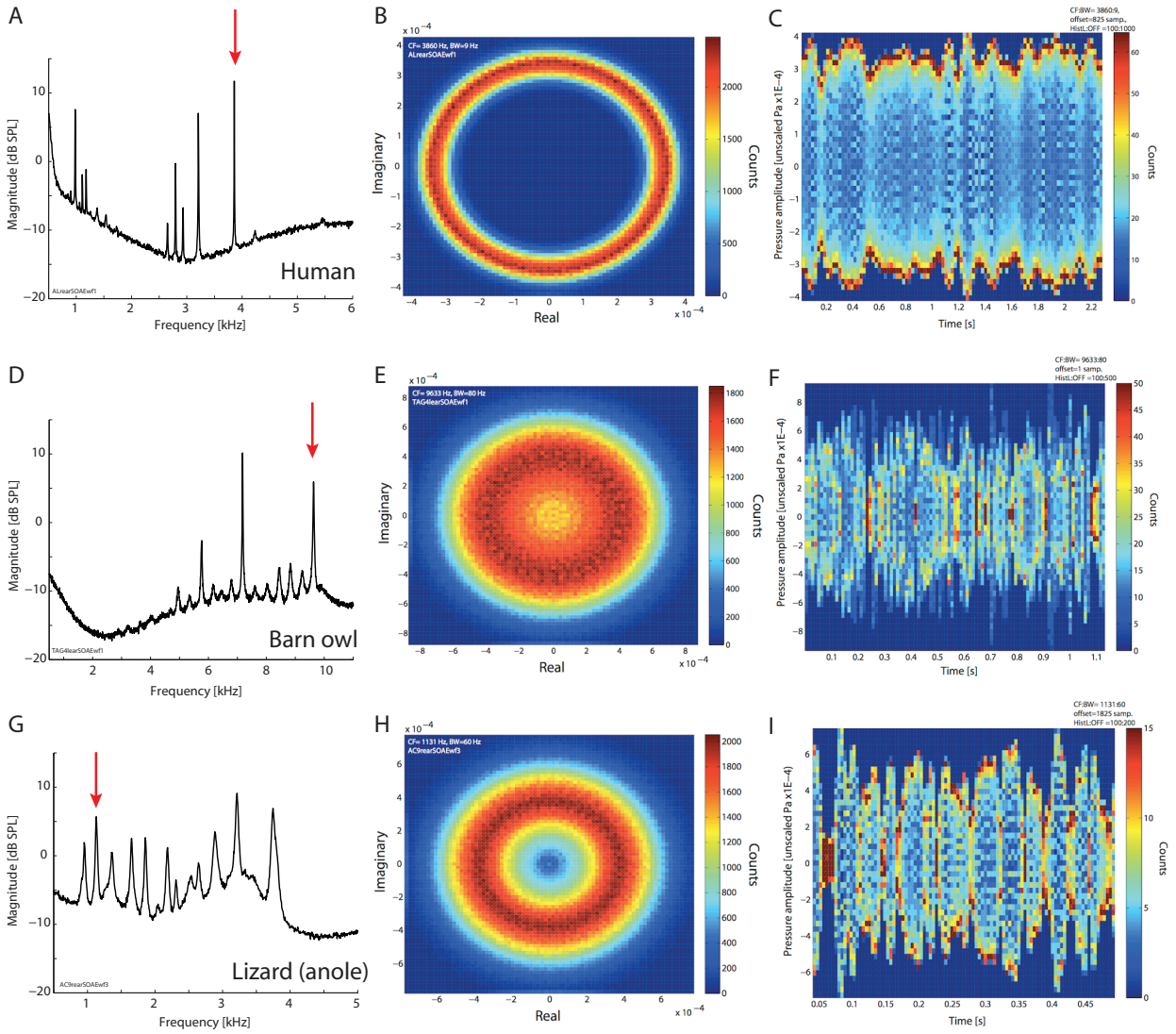

FIGURE 1. Statistical properties of a representative peak in the absence of external stimuli (see Methods). Each row shows representative individual ear for the specified species: top (A-C) – human, middle (D-F) – barn owl, bottom (G-I) – lizard. Middle column shows the distribution of the analytic signal of the filtered peak designated by the red arrow in the left column. The right column shows the amplitude distribution of that same filtered peak binned into shorter segments so to visualize the underlying dynamics (e.g., envelope fluctuations).

DISCUSSION

SOAE Classifications. We interpret the data shown in Fig.1 as supportive of the notion [12] that different classifications should exist for SOAE peaks, perhaps in part related to different 'phases' associated with relaxation dynamics [11]. For example, the barn owl shows clear SOAE activity that correlates to strong evoked OAEs (not shown here), yet clearly defined peaks possess noisier temporal characteristics compared to human or lizard. This may suggest that different coupling configurations lead to different types of collective dynamics. Such distinctions might extend beyond species and represent more general biophysical grouping of collective hair cell dynamics at work in all classes of vertebrate ears.

Entrainment dynamics. While it is presently difficult to disentangle the dynamics of the (external) tone burst and subsequent effect upon SOAEs, the precursory data and analysis reported here provide new insights. For example, note that in Fig.3F energy associated with the SOAE peak can be seen to be pulled (across frequency) towards the tone

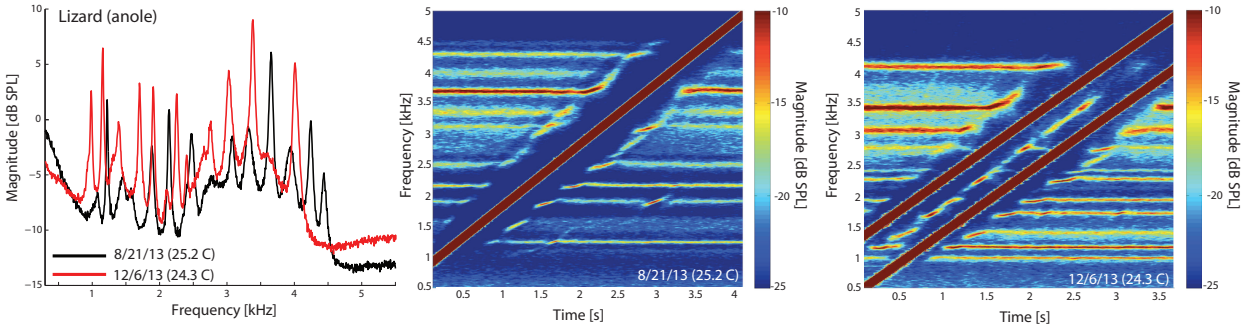

FIGURE 2. Response to swept tones. Data shown here comes from a single lizard, the same ear measured on two separate occasions. Note that body temperature was not the same for both recordings. For the 8/21/13 session (black trace in top panel), a single 45 dB SPL tone was swept across frequency (bottom left panel). For the 12/6/13 session (red trace), two 50 dB SPL tones were swept (bottom right panel) with a fixed frequency separation of 0.85 kHz. STFT analysis properties used a 8192 point window with 99% sliding overlap, spectrally averaged across 35 stimulus presentations.

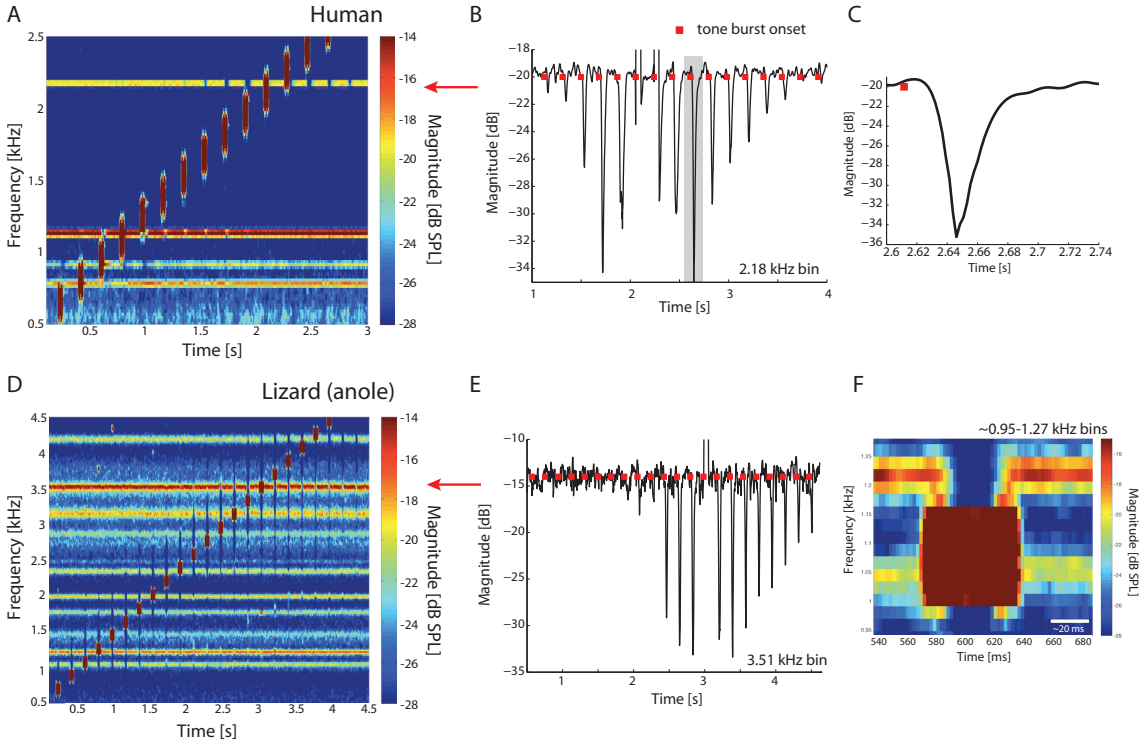

FIGURE 3. Response to tone bursts. Top row (A–C) shows response from a human ear, while bottom row (D–F) is for a lizard. Peak burst level was 60 dB SPL in both cases and used a cosine-ramping. Each presentation period containing a burst was ∼186 ms long, the human's ramped portion ∼23 ms long (i.e., 12% duty cycle) while the lizard's ramped portion was ∼45 ms long (24% duty cycle). For the human, panel B shows the waveform associated with the 2.153 kHz bin (see red arrow), with panel C zooming in upon the shaded region. Note that onset of burst is designated via a red square. For the lizard, panel E shows the waveform associated with the 3.51kHz bin. Panel F shows a zoomed in section of panel D (0.95-1.27 kHz region).

burst as it ramps up, then reverts back to its baseline during ramp down, demonstrative of an entrainment effect. Such an effect was not consistently observed though, possibly due to entrainment not always being the dominant effect (e.g., the oscillators instead being forced into a quiescent state) or the dynamics were too fast to observe given the analysis technique employed. If entrainment is present, one might use temporal ('synchronous') averaging instead to

accentuate relaxations that would subsequently dissipate via a dephasing effect.

Although preliminary, the trace shown in Fig.3C for the human suggests the possibility of two different time constants: one going into the 'suppressed' state (i.e., an entrainment time coefficient) with another returning to steady-state (i.e., a relaxation coefficient). Evidence for such in the lizard can also be seen in Fig.3D (e.g., $\sim$1.2 s mark for the 1.45 kHz peak). Furthermore, traces of the kind shown in Figs.3B and E could presumably be used in some fashion to efficiently derive 'suppression tuning curves' (e.g., [7]) and further help refine distinctions between 'iso-response' and 'iso-input' characteristics [5].

Future directions. Looking ahead, several lines of study can be pursued to clarify how the the underlying SOAE generators react to both internal and external stimuli. First, there can be improvements with regard to optimizing the time/frequency tradeoff (e.g., a different signal processing strategy rather than an overlapping STFT). Second would be study to explore how the shape of the burst affects entrainment. For example, can we distinguish to what extent the SOAE generators respond to the carrier frequency of a given burst versus dynamics (e.g., spectral splatter) associated with the envelope? Third, detailed study into inter-peak interactions (e.g., [2]) should prove valuable. Lastly, theoretical models will be essential for integrating together these various results into a coherent framework. For example, in a coupled nonlinear oscillator model, precisely what biophysical factors dictate clustering into a distinct peak versus broadband distribution as a 'baseline' emission?

ACKNOWLEDGMENTS

Supported by the Natural Sciences and Engineering Research Council of Canada (NSERC). We also thank Geoffrey Manley and Christine Köppl with regard to help collecting SOAE data from the barn owl.

REFERENCES

[1] Bialek W, Wit HP (1984) Quantum limits to oscillator stability - Theory and experiments on acoustic emissions from the human ear. Phys Lett A 104:173–178

[2] van Dijk P, Manley GA, Gallo L (1998) Correlated amplitude fluctuations of spontaneous otoacoustic emissions in six lizard species. J Acoust Soc Am 104:1559–1564

[3] van Dijk P, Manley GA, Gallo L, Pavusa A, Taschenberger G (1996) Statistical properties of spontaneous otoacoustic emissions in one bird and three lizard species. J Acoust Soc Am 100:2220–2227

[4] Epp B, Verhey JL, Mauermann M (2010) Modeling cochlear dynamics: Interrelation between cochlea mechanics and psychoacoustics. J Acoust Soc Am 128:1870

[5] Eustaquio-Martin A, Lopez-Poveda EA (2011) Isoresponse versus isoinput estimates of cochlear filter tuning. J Assoc Res Otolaryngol 12:281–299

[6] Gelfand M, Piro O, Magnasco MO, Hudspeth AJ (2010) Interactions between hair cells shape spontaneous otoacoustic emissions in a model of the tokay gecko's cochlea. PLoS ONE 5:e11116

[7] Köppl C, Manley GA (1994) Spontaneous otoacoustic emissions in the bobtail lizard. II: Interactions with external tones. Hear Res 72:159–170

[8] Long GR, Tubis A, Jones KL (1991) Modeling synchronization and suppression of spontaneous otoacoustic emissions using Van der Pol oscillators: effects of aspirin administration. J Acoust Soc Am 89:1201–1212

[9] Manley GA (2006) Spontaneous otoacoustic emissions from free-standing stereovillar bundles of ten species of lizard with small papillae. Hear Res 212:33–47

[10] Shera CA (2003) Mammalian spontaneous otoacoustic emissions are amplitude-stabilized cochlear standing waves. J Acoust Soc Am 114:244–262

[11] Sisto R, A M, M L (2001) Spontaneous otoacoustic emissions and relaxation dynamics of long decay time OAEs in audiometrically normal and impaired subjects. J Acoust Soc Am 109:638–647

[12] Talmadge CL, Tubis A, Wit HP, Long GR (1991) Are spontaneous otoacoustic emissions generated by self-sustained cochlear oscillators? J Acoust Soc Am 89:2391–2399

[13] Wit HP (1986) Statistical properties of a strong otoacoustic emission. In: Allen J (ed) Peripheral Auditory Mechanisms, Springer-Verlag, pp. 221–228

[14] Wit HP, van Dijk P (2012) Are human spontaneous otoacoustic emissions generated by a chain of coupled nonlinear oscillators? J Acoust Soc Am 132:918–926

[15] Zwicker E, Schloth E (1984) Interrelation of different otoacoustic emissions. J Acoust Soc Am 75:1148–1154